pISSN 1598-2998, eISSN 2005-9256
https://doi.org/10.4143/crt.2024.780 Cancer Res Treat. 2025;57(3):803-820

Original Article

Identifying Anti-cancer Effects and Exploring the Mechanism of an MPS1/TTK Inhibitor in Gastric Cancer

Eunseo Kim[1,2], **Woo Sun Kwon**[1], **Tae Soo Kim**[1], **Jihyun Hwang**[1,2], **Sunghwan Kim**[3], **Sun Young Rha**[1,2,4,5]

[1]*Song-Dang Institute for Cancer Research, Yonsei University College of Medicine, Seoul,* [2]*Brain Korea 21 PLUS Project for Medical Science, Yonsei University College of Medicine, Seoul,* [3]*Voronoi Inc., Incheon,* [4]*Department of Medicine, Yonsei University College of Medicine, Seoul,* [5]*Division of Medical Oncology, Department of Internal Medicine, Yonsei Cancer Center, Yonsei University Health System, Seoul, Korea*

Purpose This study aimed to identify the anti-cancer effect and investigate the underlying mechanism of MPS1/TTK (monopolar spindle 1; also known as threonine tyrosine kinase) inhibitor in gastric cancer (GC) cell lines.

Materials and Methods This study used compound-9, a highly selective MPS1/TTK inhibitor, to evaluate its anti-cancer effects on GC cell lines. Cell viability assay was performed to determine sensitivity to the inhibitor. Cell cycle analysis and apoptosis assays were performed using Flow cytometry to evaluate the effects of the inhibitor. Protein-expression levels were analyzed through western blotting after the inhibitor treatment.

Results The Epstein-Barr virus and microsatellite-instable–high groups tended to be sensitive to the inhibitor, while the genomically stable (GS)–likely group tended to be moderate-to-resistant. In contrast, the chromosomal instability (CIN)–likely group was extremely sensitive or resistant. Within the CIN group, $TP53^{WT}$ cell lines were sensitive, whereas $TP53^{MUT}$ cell lines were sensitive or resistant. Upon treatment of the inhibitor, the $TP53^{WT}$-sensitive cell line underwent cell death more rapidly compared to the $TP53^{MUT}$-sensitive cell line. In contrast, the $TP53^{MUT}$-sensitive cell experienced higher levels of aneuploidy or polyploidy and underwent cell death at later time point than the $TP53^{WT}$-sensitive cell line. The $TP53^{MUT}$-resistant line can tolerate aneuploidy or polyploidy and exhibits drug resistance.

Conclusion Our study explores the potential of an MPS1/TTK inhibitor, compound-9, as a targeted therapy in GC cells and investigates its mechanism of action.

Key words Stomach neoplasms, Chromosome instability, MPS1 inhibitor, SAC pathway

Introduction

Gastric cancer (GC) is the fifth most common cancer and the fourth leading cause of cancer death worldwide, with a particularly high incidence in East Asia [1,2]. Despite advances in the early detection and treatment of GC, most patients are diagnosed at an advanced stage and systemic chemotherapy has a poor prognosis with a median overall patient survival of approximately 14 months [3]. Therefore, there is an urgent need for new targeted molecular therapies that can effectively treat GC.

Chromosomal instability (CIN) is one of the hallmarks of human cancer and an attractive therapeutic target [4]. CIN refers to an increased rate of chromosome mis-segregation due to errors in mitosis. One of the main products of CIN is aneuploidy, a condition associated with the gain or loss of whole chromosomes or parts leading to genomic imbalances [5]. CIN is a common feature of cancer cells, but even these cells cannot tolerate aneuploidy above a certain threshold, and excessive CIN could induce tumor cells death [6]. Therefore, the immediate generation of unsustainable CIN is an attractive area for cancer therapeutic intervention.

Spindle assembly checkpoint (SAC) is one of the CIN-tolerance mechanisms to prevent cell death, ensuring proper chromosome segregation during mitosis [7,8]. SAC monitors the correct bipolar attachment and tension of microtubules (MT). If there is no attachment between the chromosomes and MTs, the anaphase promoting complex/cyclosome (APC/C) is inactivated, which delays entry into anaphase until the kinetochores are properly attached. Activation of the SAC requires the assembly of the mitotic checkpoint complex (MCC) and a number of proteins [8]. Monopolar spindle 1 (MPS1) kinase (also known as threonine tyrosine kinase; TTK) is a key protein of SAC, essential for the recruitment of the MCC and MPS1/TTK is overexpressed in breast, glioma, liver, lung, pancreatic, thyroid cancer, and GC [9-17]. Thus,

Correspondence: Sun Young Rha
Song-Dang Institute for Cancer Research, Division of Medical Oncology, Department of Internal Medicine, Yonsei Cancer Center, Yonsei University College of Medicine, 50-1 Yonsei-ro, Seodaemun-gu, Seoul 03722, Korea
Tel: 82-2-2228-8050 E-mail: rha7655@yuhs.ac
Received August 14, 2024 **Accepted** December 10, 2024 **Published Online** December 12, 2024

generation of chromosome segregation errors and deleterious aneuploidies induced by MPS/TTK inhibition represents an attractive target for therapeutic intervention in cancer.

The cells eventually exit mitosis, following abnormal sister chromatid segregation and cytokinesis induced by MPS1/TTK inhibitor, and enter G1 phase with accumulation of CIN [18,19]. In p53-competent cells, these cells either arrest in G1 or undergo p53-dependent cell death, called post-mitotic checkpoint. Cells deficient in p53 survive by continuing to proliferate and replicate DNA [20,21]. Thus, the activation of p53 prevents further DNA replication and polyploidy by inducing cell death.

In this study, we performed integrated molecular profiling of MPS1/TTK and TP53 and evaluated the preclinical efficacy of the MPS1/TTK inhibitor according to TP53 status in 61 GC cell lines.

Materials and Methods

1. Materials

MPS1/TTK inhibitor, compound-9, is a highly selective MPS1 inhibitor based on a 7H pyrrolopyrimidine-5-carbonitrile scaffold. Compound-9 exhibits remarkable selectivity and efficacy, particularly showcasing significant anti-cancer effects in triple-negative breast cancer models [22].

2. Cell lines and cultures

Among the 61 human GC cell lines, 38 of cell lines were established by Song-Dang Institute for Cancer Center and 23 of cell lines were purchased at three different organizations worldwide (American Type Culture Collection, Korean Cell Line Bank and Japanese Collection of Research Bioresources Cell Bank). Cell lines were maintained using their proper complete growth medium. Basically, Eagle's minimum essential medium, Dulbecco's modified Eagle medium and Roswell Park Memorial Institute-1640 (RPMI-1640) (Gibco) contained 1% of antibiotics (Lonza) and 5% of fetal bovine serum (Lonza) were consumed for the maintenance of cell lines. Cell lines were grown at 37°C in 5% CO_2 incubator.

3. Genomic profiling

In-house targeted deep sequencing (CancerMaster), whole exome sequencing (WES) and RNA sequencing data of the 61 GC cell lines were obtained from the genome database of Song-dang Institute for Cancer Research (SICR), Yonsei University College of Medicine [23,24]. TP53, receptor tyrosine kinases (RTKs) (MET, fibroblast growth factor receptor 2, ERBB2, epidermal growth factor receptor), and DNA damage repair (DDR)–related genes were analyzed using CancerMaster [23,25]. MPS1/TTK was analyzed by WES. The mRNA expression levels were measured in transcripts per kilobase million (TPM) without normalization. The GC cell lines were classified according to The Cancer Genome Atlas (TCGA) subgroups based on CancerMaster [23,25]. The 61 GC cell lines were grouped as Epstein-Barr virus (n=2, 3.3%), microsatellite-instable–high (MSI-H; n=4, 6.6%), CIN-likely (n=27, 44.3%), and genomically stable (GS)–likely (n=28, 46.0%) (Fig. 1). In this paper, the CIN and GS types suggested by TCGA are stated as CIN-likely and GS-likely. The 61 GC cell lines used in this study cannot be categorized by the same method as TCGA and we used the gene signature of CIN and GS group presented by TCGA for classification. The tumor mutation burden (TMB) was examined using CancerMaster. The TMB ranged from 2.9 to 63.2, with a median of 10.2. The biological effects of different mutations were assessed using the OncoKB database (https://www.oncokb.org/).

4. Cell viability assay

The cells (8×10^3/well) were seeded in 96-well plates overnight at 37°C and exposed to specific doses of MPS1/TTK inhibitor (0-10 μM) at 37°C for 72 hours. Cell Counting Kit-8 (Dojindo) solution was added, and the plates were incubated at 37°C for a further 2 hours. The absorbance was measured at 450 nm and IC_{50} values were determined using the CalcuSyn software (Biosoft). The cell lines were divided into sensitive, moderate, and resistant groups using the IC_{50} values. All experiments were repeated three times.

5. Western blotting

Cells were lysed in the M-PER mammalian protein extraction reagent (Pierce) containing phosphatase inhibitor (Sigma) and protease inhibitor (Roche). Protein concentrations were determined by the Bradford Assay (Bio-Rad). Proteins were separated by 8%-15% sodium dodecyl sulfate polyacrylamide gel electrophoresis and transferred to polyvinylidene difluoride membranes. Non-specific antibody binding was reduced by blocking process with 5% skim milk at 1hrs incubation. Membranes were incubated overnight at 4°C with following primary antibodies: cyclinB1 (sc-245, Santa Cruz Biotech), phospho-histone H2A.X (γ-H2AX) (Ser139) (9718S, Cell Signaling), $p21^{WAF1}$ (OP64, Calbiochem), BUBR1 (612503, BD Biosciences), phospho-BUBR1 (612503, BD Biosciences), MPS1/TTK (35-9100, Invitrogen), and α-tubulin (T6199, Sigma). After 6 times of wash, membranes were incubated for 2 hours at room temperature with horseradish peroxidase–conjugated secondary antibody. anti-mouse (1706516, Bio-Rad) or anti-rabbit (1721019, Bio-Rad) antibodies were used as secondary antibodies. Immunoblots were developed using LumiFlash Ultima Chemiluminescent Substrate (Visual Protein) and visualized by ChemiDoc XRS+ system (Bio-Rad). Data were normalized to α-tubulin, and

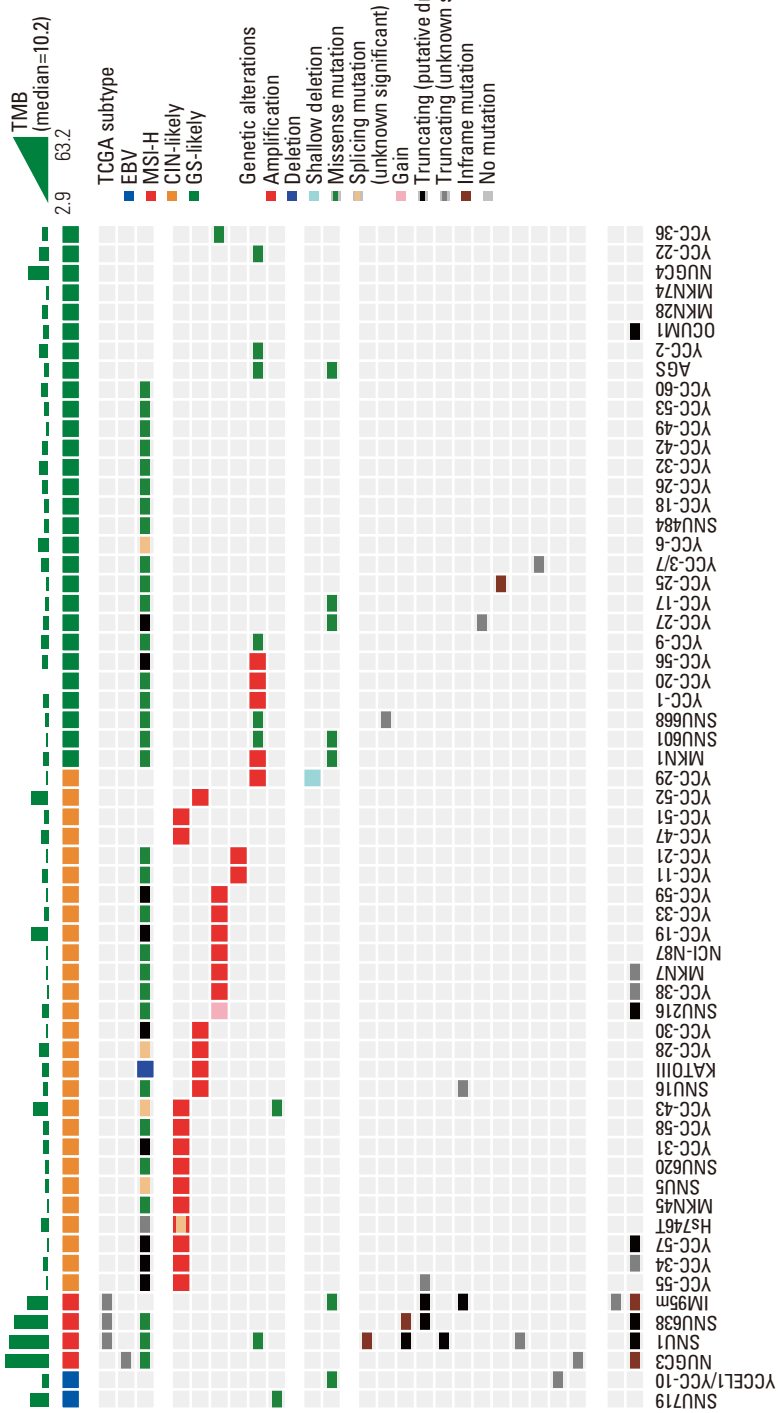

Fig. 1. Molecular-genomic profiling in 61 gastric cancer (GC) cell lines. Tumor mutation burden (TMB) was counted as the total number of somatic mutations by next-generation sequencing, The Cancer Genome Atlas (TCGA) subtype of 61 GC cell lines and landscape of monopolar spindle 1 (MPS1)/threonine tyrosine kinase (TTK), TP53, receptor tyrosine kinase (RTK)–RAS, phosphoinositide 3-kinase (PI3K), and DNA damage repair–related genes with genetic alterations. CIN, chromosomal instability; EBV, Epstein-Barr virus; GS, genomically stable; HR, homologous recombination; MSI-H, microsatellite-instable–high; NHEJ, non-homologous end joining.

Table 1. MPS1/TTK inhibitor sensitivity group's distribution by genomic profiling

		Total (n=61)	Sensitive (≤ 0.1 μM) (n=21)	Moderate (> 0.1 and < 10 μM) (n=23)	Resistan (≥ 10 μM) (n=17)	p-value
TCGA subgroup	EBV (n=2)		1 (50.0)	1 (50.0)	0	-
	MSI-H (n=4)		3 (75.0)	1 (25.0)	0	-
	CIN-likely (n=27)		13 (48.2)	5 (18.5)	9 (33.3)	0.005
	GS-likely (n=28)		4 (14.8)	16 (57.1)	8 (28.6)	
TMB (mut/Mb)	TMB-H (≤ 20) (n=9)		5 (23.8)	1 (4.3)	3 (17.6)	0.002
	TMB-L (< 20) (n=52)		16 (76.2)	22 (95.7)	14 (82.4)	
TP53 status	Wild type (n=15)		7 (47.0)	5 (33.0)	3 (20.0)	0.001
	Mutant type (n=46)		14 (30.0)	18 (40.0)	14 (30.0)	
TP53 status in CIN-likely group (n=27)	Wild type (n=4)		3 (75.0)	1 (25.0)	0	-
	Mutant type (n=23)		10 (43.0)	4 (17.0)	9 (39.0)	-
DDR-related genes	Wild type (n=44)		15 (34.0)	15 (34.0)	14 (32.0)	
	Mutant type (n=17)		6 (35.0)	8 (47.0)	3 (18.0)	
DDR-related genes in *TP53* wild type (n=15)	Wild type (n=12)		6 (50.0)	3 (25.0)	3 (25.0)	
	Mutant type (n=3)		1 (33.3)	2 (66.7)	0	
DDR-related genes in *TP53* mutant type (n=46)	Wild type (n=32)		9 (28.0)	12 (38.0)	11 (34.0)	0.779
	Mutant type (n=14)		5 (36.0)	6 (43.0)	3 (21.5)	
RTK gene amplification or gain in	MET (n=12)		9 (75.0)	2 (17.0)	1 (8.0)	-
CIN-likely (n=26/27)	FGFR2 (n=5)		3 (60.0)	0	2 (40.0)	-
*1 cell line: PTEN deletion	ERBB2 (n=7)		0	2 (29.0)	5 (71.0)	-
	EGFR (n=2)		1 (50.0)	0	1 (50.0)	-

Values are presented as number (%). CIN, chromosomal instability; DDR, DNA damage repair; EBV, Epstein-Barr virus; GS, genomically stable; MPS1, monopolar spindle 1; MSI-H, microsatellite-instable–high; RTK, receptor tyrosine kinase; TCGA, The Cancer Genome Atlas; TMB, tumor mutation burden; TTK, threonine tyrosine kinase.

protein intensity was semi-quantified using the ImageJ software (NIH). All experiments were repeated three times and quantification was performed with ImageJ using α-tubulin as loading control.

6. Cell cycle analysis

Cells (1×10^6/well) were seeded in 60-mm cell culture dishes overnight at 37°C, treated with 0.05, 0.5, and 1 μM MPS1/TTK inhibitor for 12, 24, 48, and 72 hours and harvested with 0.25% trypsin/EDTA (Gibco), before being fixed with cold 75% ethanol at −20°C for at least 24 hours. Next, cells were washed twice with cold phosphate buffered saline (PBS), and stained with propidium iodide/RNase Staining Buffer (BD Pharmingen) for 20 minutes in the dark at 20°C. Cell cycle distribution was analyzed using a BD LSRII (BD Pharmingen) and the Flow Jo software (Tristar). All experiments were repeated three times.

7. Apoptosis assay

Cells (1×10^6/well) were seeded in 60-mm cell culture dishes and incubated for 24 hours. Cells were then treated with drugs for 12 and 24 hours and the supernatant (containing floating death cells) and adherent cells were collected together. The collected cells were washed twice with PBS, then centrifuged. The pellet was resuspended in 100 μL of AnnexinV binding buffer and stained using BD AnnexinV/FITC apoptosis kit (BD Biosciences). Apoptotic cells were measured using flow cytometry. All experiments were repeated three times.

8. Statistical analysis

All assays were performed independently at least three times unless indicated. Mean with standard error mean was represented in each graph. IBM SPSS Statistics for Windows ver. 27.0 software (IBM Corp.) was used for statistical analysis including correlation analysis, paired, non-paired t tests, correlation coefficient, and chi-square test.

Results

1. Molecular-genomic profiling of 61 GC cell lines

We profiled the status of MPS1/TTK, TP53, and DDR-related genes (Fig. 1). Frameshift mutation at coding mon-

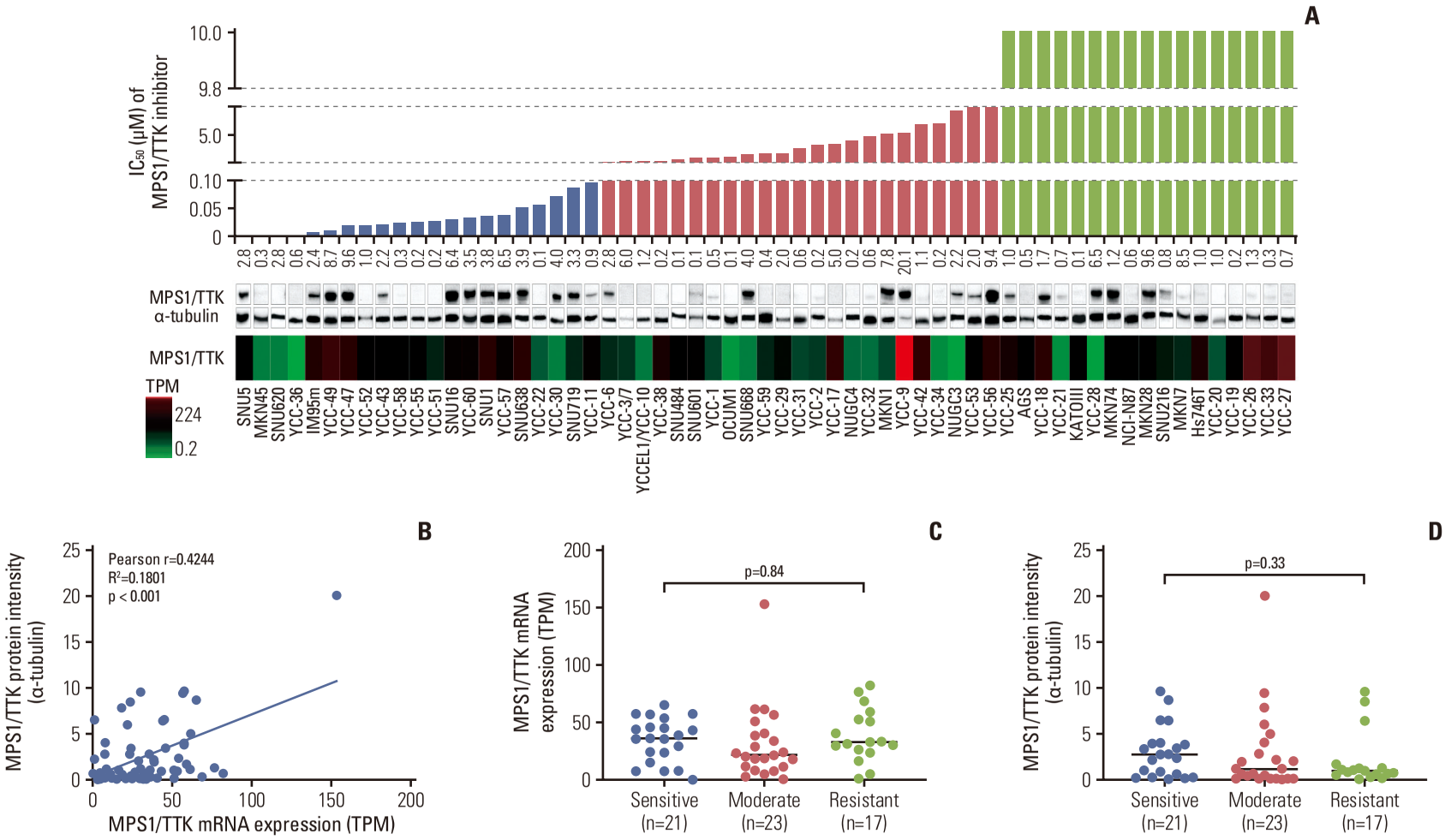

Fig. 2. Monopolar spindle 1 (MPS1)/threonine tyrosine kinase (TTK) inhibitor sensitivity in 61 gastric cancer cell lines. (A) At the top panel, Waterfall plots representing IC_{50} (μM) values for each cell lines determined using the CalcuSyn software (color-coded as per the legend: sensitive, blue [0.1 μM ≤ IC_{50}]; moderate, red [0.1 μM < IC_{50} < 10 μM]; resistant, green [IC_{50} ≥ 10 μM]). At the middle panel, Protein expression of MPS1/TTK was determined by western blotting with α-tubulin as loading control and compared to YCC-25. Quantification of each protein levels is indicated on the band above. At the bottom panel, mRNA expression was analyzed using RNA sequencing data and is color-coded according to the heatmap legend. (B) Correlation between MPS1/TTK mRNA expression level (transcripts per kilobase million [TPM]) and MPS1/TTK protein expression. (C) Association between MPS1/TTK inhibitor sensitivity and MPS1/TTK mRNA expression level (TPM). (D) Association between MPS1/TTK inhibitor sensitivity MPS1/TTK protein expression (unpaired t test with Welch's correction between sensitive and resistant group). *(Continued to the next page)*

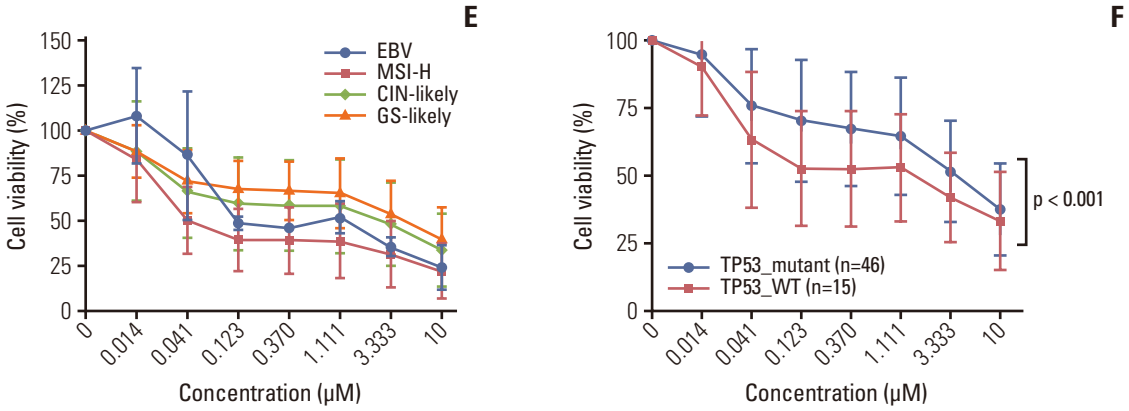

Fig. 2. *(Continued from the previous page)* (E) Dose-response curves for the 61 gastric cancer (GC) cell lines according to The Cancer Genome Atlas subtype. MPS1/TTK inhibitor cytotoxicity was evaluated using Cell Counting Kit-8 assays and is expressed as the mean percentage cell viability according to The Cancer Genome Atlas subtype (color-coded as per the legend: Epstein-Barr virus [EBV], blue; microsatellite-instable–high [MSI-H], red; genomically stable (GS)–likely, orange; chromosomal instability [CIN]–like, green). (F) Dose-response curves for the 61 GC cell lines according to TP53 status (color-coded as per the legend: TP53_wild type [WT], red; TP53_mutant, blue). The statistical tests performed with chi-square test and data are expressed as mean±standard error of mean.

onucleotide repeats (cMNR) in the MPS1/TTK gene were observed in four of the 61 cell lines (6.6%) using WES, all of which belonged to the MSI-H subgroup. These cMNR mutations are known to result in the production of truncated MPS1/TTK proteins and occur at a high frequency in microsatellite-instable (MSI) colorectal cancer and GC [26]. The mRNA level of MPS1/TTK is expressed at low levels (0.2-153 TPM). However, the mRNA and protein expression levels of MPS1/TTK showed a moderate correlation in 61 GC cell lines (R^2=0.1801, $p < 0.001$).

According to in-house deep sequencing, 46 GC cell lines (75%) containing *TP53* alterations (32 missense mutations, 11 truncating mutations, or 4 splicing variants) were discovered. Moreover, we also checked any alterations of DDR-related gene changes which are based on 35 genes that involved in two mechanisms of double-strand break repair, homologous recombination and non-homologous end joining (Fig. 1) [27]. As a result, we confirmed 17 GC cell lines (28%) had DDR alterations (Table 1). Based on 61 GC cell lines genomic profiling, we performed experiments to identify anti-cancer effect and explore the mechanisms of MPS1/TTK inhibitor in the GC cell lines.

2. Anti-proliferative effects of the MPS1/TTK inhibitor in 61 GC cell lines

Next, we evaluated the effects of the MPS1/TTK inhibitor in 61 GC cell lines. We confirmed cell line viability to check the sensitivity of the MPS1/TTK inhibitor. Moreover, we classified the cell lines according to their IC_{50} values, ranged from 0.002 μM to ~10 μM, with a median value of 1.80 and a mean value of 4.15 (Fig. 2A, S1 Fig.). Cell lines were classified into three groups: sensitive ($IC_{50} \geq 0.1$ μM), moderate (0.1 μM $< IC_{50} <$ 10 μM), and resistant ($IC_{50} \geq 10$ μM). As a result, the viability of 61 cell lines treated with the MPS1/TTK showed that 34% (n=21) of the cell lines were sensitive, 38% (n=23) were moderate, and 28% (n=17) were resistant to the inhibitor (Table 1).

3. Association between molecular-genomic profiling and sensitivity to the MPS1/TTK inhibitor

Next, we compared the sensitivity of 61 GC cell lines to MPS1/TTK inhibitor with the previous molecular-genomic profiling data in Fig. 1. There was no correlation observed between IC_{50} values and MPS1/TTK mRNA or protein expressions not like inhibitor treatment (Fig. 2B-D). Next, we compared sensitivity to the MPS1/TTK inhibitor according to the TCGA subtype (Fig. 2E). Of the four cell lines in the MSI-H group, three were sensitive (75%), and one was moderately sensitive (25%). Of the 27 cell lines in the CIN-likely group, 13 cell lines were sensitive (48.2%), five cell lines were moderate (18.5%), and nine cell lines were resistant (33.3%). Of the 28 cell lines in the GS-likely group, four cell lines were sensitive (14.8%), 16 cell lines were moderate (57.1%), and eight cell lines were resistant (28.6%). Intriguingly, MSI-H group was highly sensitive to MPS1/TTK inhibitor. This result consistent with previous reports of high sensitivity to the MPS1/TTK inhibitor in MSI colorectal cancers [26].

The GS-likely group tended to be moderate-to-resistant, whereas the CIN-likely group was extremely sensitive or resistant to the MPS1/TTK inhibitor. The CIN-likely group was more sensitive than the GS-likely group (chi-squared p=0.0051) (Table 1). Based on this, we investigated the dif-

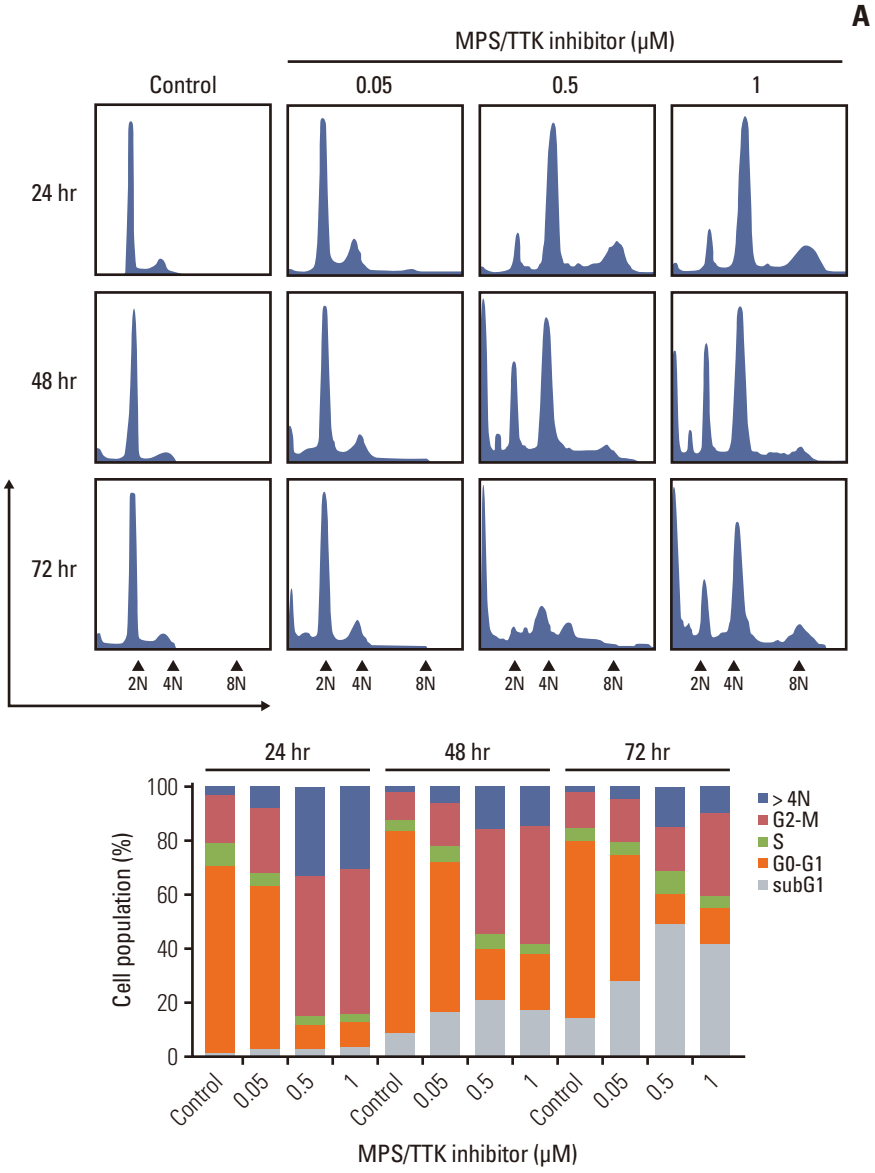

Fig. 3. Effect of the monopolar spindle 1 (MPS1)/threonine tyrosine kinase (TTK) inhibitor on cell-cycle progression. Effect of the MPS1/TTK inhibitor on cell-cycle progression in YCC-47 ($TP53^{WT}$, sensitive) cell line (A), YCC-30 ($TP53^{MUT}$, sensitive) cell line (B), and YCC-28 ($TP53^{MUT}$, resistant) cell line (C). At the upper panel, histograms of cell cycle analysis after treatment with the MPS1/TTK inhibitor were represented (The y-axis represents cell counts, and the x-axis represents DNA modal contents). At the lower panel, cell cycle distribution bar graph (The y-axis represents the percentage of cell population, and the x-axis represents the conditions) was represented. *(Continued to the next page)*

ferences in cell lines that were sensitive or resistant to the MPS1/TTK inhibitor in the CIN-likely group.

Next, we examined TP53 status to identify its influence on the response to the MPS1/TTK inhibitor (Fig. 2F). The $TP53^{WT}$ group was more sensitive than the $TP53^{MUT}$ group (chi-squared $p < 0.001$) (Table 1). This suggests that deleterious CIN induced by the MPS1/TTK inhibitor triggers detection by p53, leading to cell death in p53-competent cells [20]. Interestingly, $TP53^{WT}$ and CIN-likely GC cell lines were sensitive to the MPS1/TTK inhibitor, whereas $TP53^{MUT}$ and CIN-likely GC lines were sensitive or resistant (Table 1). From these results, MPS1/TTK resistant and sensitive cell lines based on TP53 status in the CIN-likely group were selected for further studies.

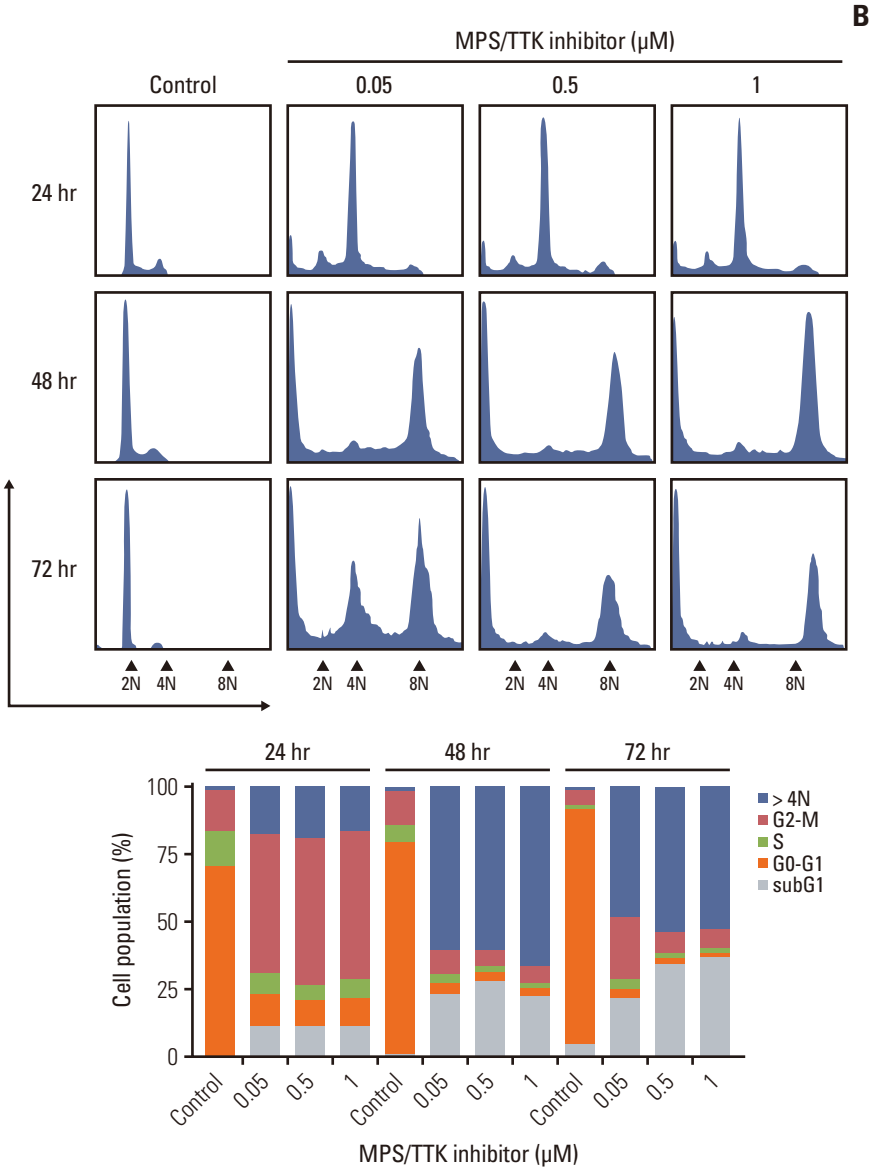

Fig. 3. *(Continued from the previous page)* *(Continued to the next page)*

4. Effect of the MPS1/TTK inhibitor on cell-cycle progression

We investigated the effects of MPS1/TTK inhibitor treatment on cell-cycle progression and genomic instability using flow cytometry on YCC-47 (IC_{50}=0.02 μM, sensitive, $TP53^{WT}$), YCC-30 (IC_{50}=0.07 μM, sensitive, $TP53^{MUT}$), and YCC-28 (IC_{50} > 10 μM, resistant, $TP53^{MUT}$) cell lines (Fig. 3).

After 24 hours of treatment, all three cell lines showed a reduction in the percentage of cells in the G0/G1 phase, with an increase in the G2/M phase and aneuploidy or polyploidy (> 4N) (Fig. 3A-C). However, this increase was most pronounced in YCC-47, the most sensitive cell line (Fig. 3A). After 48 hours of treatment, the YCC-47 cell line had less aneuploid or polyploid (> 4N ploidy) than before 24 hours of treatment, with a significant increase in the sub-G1 phase (Fig. 3A). In contrast, YCC-28 cells remained mostly in the G2-M phase and still developed aneuploidy and polyploidy (> 4N), similar to the 24-hour treatment (Fig. 3C). The YCC-30 cell line showed a significant increase in 8N ploidy compared to the other two cell lines (Fig. 3B). After 72 hours of treatment, the YCC-47 cell line showed concentration-dependent cell cycle collapse, with an increase in the sub-G1 phase (Fig. 3A). In YCC-30, the majority of cells had shifted towards 8N polyploidy and sub-G1 phase, whereas YCC-28 continued to

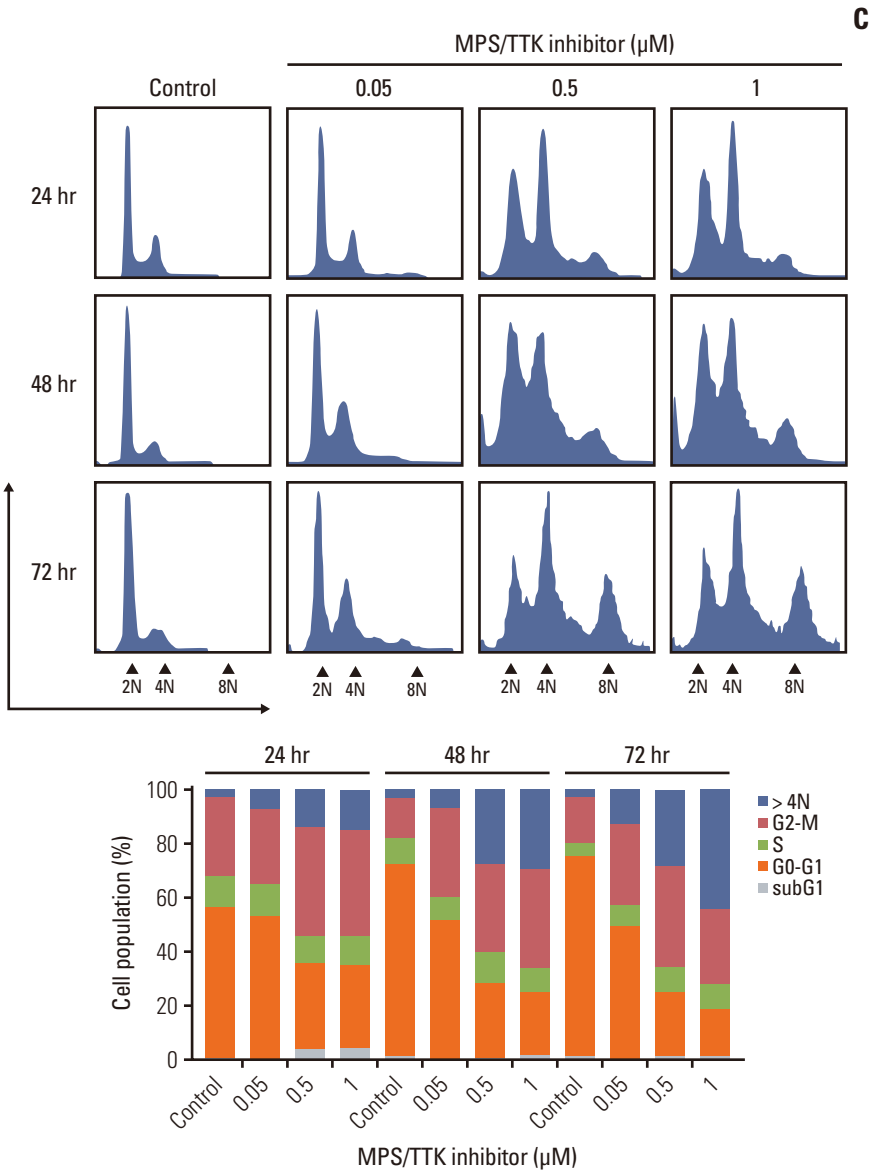

Fig. 3. *(Continued from the previous page)*

exhibit resistance, with most cells remaining in G2/M and showing no increase in subG1 (Fig. 3B and C).

These results suggest that MPS1/TTK inhibition leads to rapid apoptosis in sensitive cell lines like YCC-47, whereas resistant lines like YCC-28 can tolerate aneuploidy and polyploidy, contributing to their drug resistance. YCC-30 shows a delayed response, eventually leading to cell death through polyploidy.

5. Changes in molecular factors and cell death induced by the MPS1/TTK inhibitor

To explore further mechanisms of the MPS1/TTK inhibitor to the YCC-47, YCC-30, and YCC-28 cell lines, we checked protein expression of MPS1/TTK, cyclin B1, γ-H2AX, and p21 after 24- or 48-hours treatment at concentrations of 0.05, 0.5, or 1 (Fig. 4).

First, MPS1/TTK expression levels decreased in YCC-47 and YCC-30 cells in a time- and concentration-dependent manner (Fig. 4A, B, D, and E). However, in YCC-28 cells, MPS1/TTK levels remained unchanged across all concentrations (Fig. 4C and F), indicating resistance to the inhibitor in this cell line. Second, the cyclin B1, a substrate of APC/C, exhibited different patterns of regulation across the cell lines. YCC-30 cells showed a significant reduction in cyclin B1

after 24 hours of treatment at 1 μM (Fig. 4B and E). In contrast, YCC-47 (Fig. 4A and D) and YCC-28 (Fig. 4C and F) cell lines demonstrated increased cyclin B1 levels after the same treatment. By 48 hours, cyclin B1 levels continued to decrease in YCC-47 cell line (Fig. 4A and D), while YCC-28 cell line (Fig. 4C and F) exhibited a concentration-dependent decline in cyclin B1 expression. Third, γ-H2AX, a marker of DNA damage, showed an increase in both YCC-47 and YCC-30 cells after treatment with the MPS1/TTK inhibitor (Fig. 4A, B, D, and E). This suggests that DNA damage accumulation was induced by MPS1/TTK inhibition in the more sensitive cell lines. At last, p21 expression was increased in the $TP53^{WT}$ YCC-47 (Fig. 4A and D) cell line upon treatment with the MPS1/TTK inhibitor. However, this increase was not observed in the $TP53^{MUT}$ cell lines, YCC-30 and YCC-28 (Fig. 4B, C, E, and F).

These results suggest that YCC-47 and YCC-30 cells undergo significant DNA damage accumulation in response to MPS1/TTK inhibition, as evidenced by increased γ-H2AX levels and cell cycle arrest at the G2/M phase. In contrast, YCC-28 cells exhibited resistance to the inhibitor, with no significant changes in DNA damage markers or cell cycle progression, further indicating their resistance to MPS1/TTK inhibition.

6. Apoptosis induced by the MPS1/TTK inhibitor

The effect of the MPS1/TTK inhibitor on the apoptosis was determined by apoptosis assay (Fig. 5). Percentage of apoptotic cells increased significantly in the YCC-47 (Fig. 5A and D) or YCC-30 (Fig. 5B and E) cell lines in a concentration- and time-dependent manner, whereas YCC-28 (Fig. 5C and F) cell line does not show any increase. Additionally, the YCC-47 cell line exhibited a high proportion of apoptotic cells, while the YCC-30 cell line had a high proportion of necrotic cells, suggesting that cell death occurred through different mechanisms in these two cell lines.

These results suggest that DNA damage accumulated in a time- and concentration-dependent manner in YCC-47 and YCC-30 cell lines, leading to DNA damage stress-induced cell death. Additionally, the post-mitotic checkpoint was activated in the YCC-47 cell line upon MPS1/TTK inhibitor treatment, but not in YCC-30 cells, suggesting that cell death occurred through different mechanisms in the YCC-47 and YCC-30 cell lines.

7. Differential cell cycle recovery after SAC activation in YCC-47 and YCC-28 cell lines following MPS1/TTK inhibition

We next examined the impact of the MPS1/TTK inhibitor on the SAC activity in $TP53^{WT}$ (YCC-47) and $TP53^{MUT}$ (YCC-28) cells lines. SAC activity was induced by treating cells with nocodazole, a MT depolymerizer, which arrests cells in the G2/M phase by generating unattached kinetochores (Fig. 6).

Analysis of cell cycle distribution showed that both YCC-47 (Fig. 6A) and YCC-28 (Fig. 6B) cells were arrested in the G2/M phase upon nocodazole treatment. Notably, YCC-47 cells displayed a higher proportion of polyploid cells (> 4N) when arrested with nocodazole compared to YCC-28 cells.

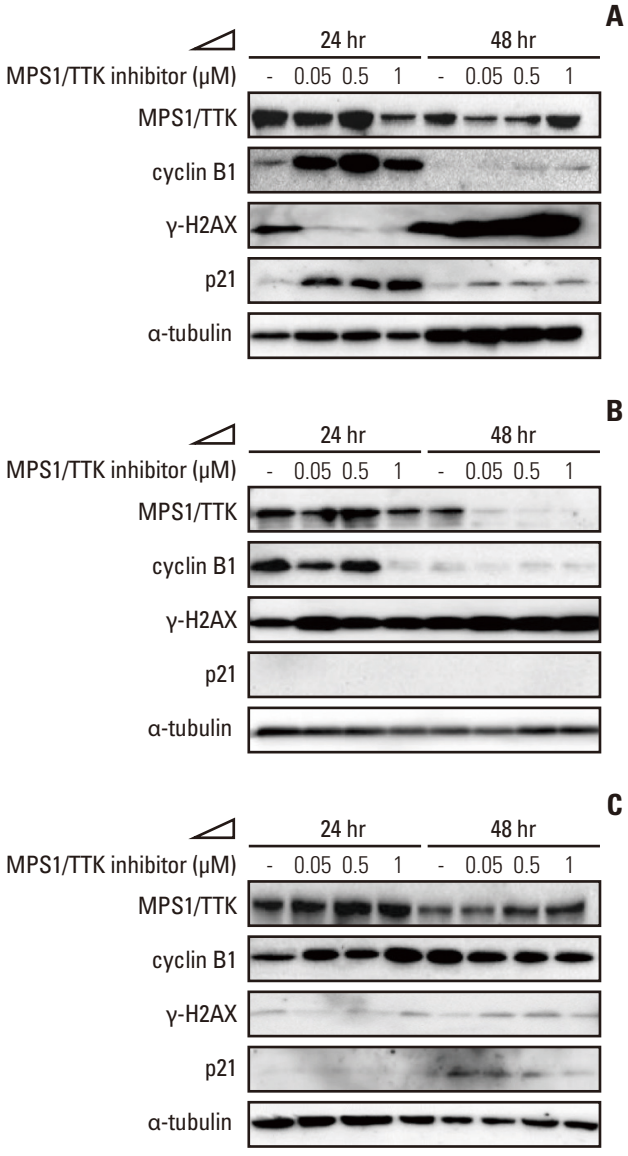

Fig. 4. Changes in molecular factors and cell death induced by the monopolar spindle 1 (MPS1)/threonine tyrosine kinase (TTK) inhibitor. Protein expression of MPS1/TTK, cyclin B1, γ-H2AX, and p21 after 24- or 48-hour treatment with 0.05, 0.5, or 1 μM of the MPS1/TTK inhibitor in YCC-47 cell line (A), YCC-30 cell line (B), and YCC-28 cell line (C). *(Continued to the next page)*

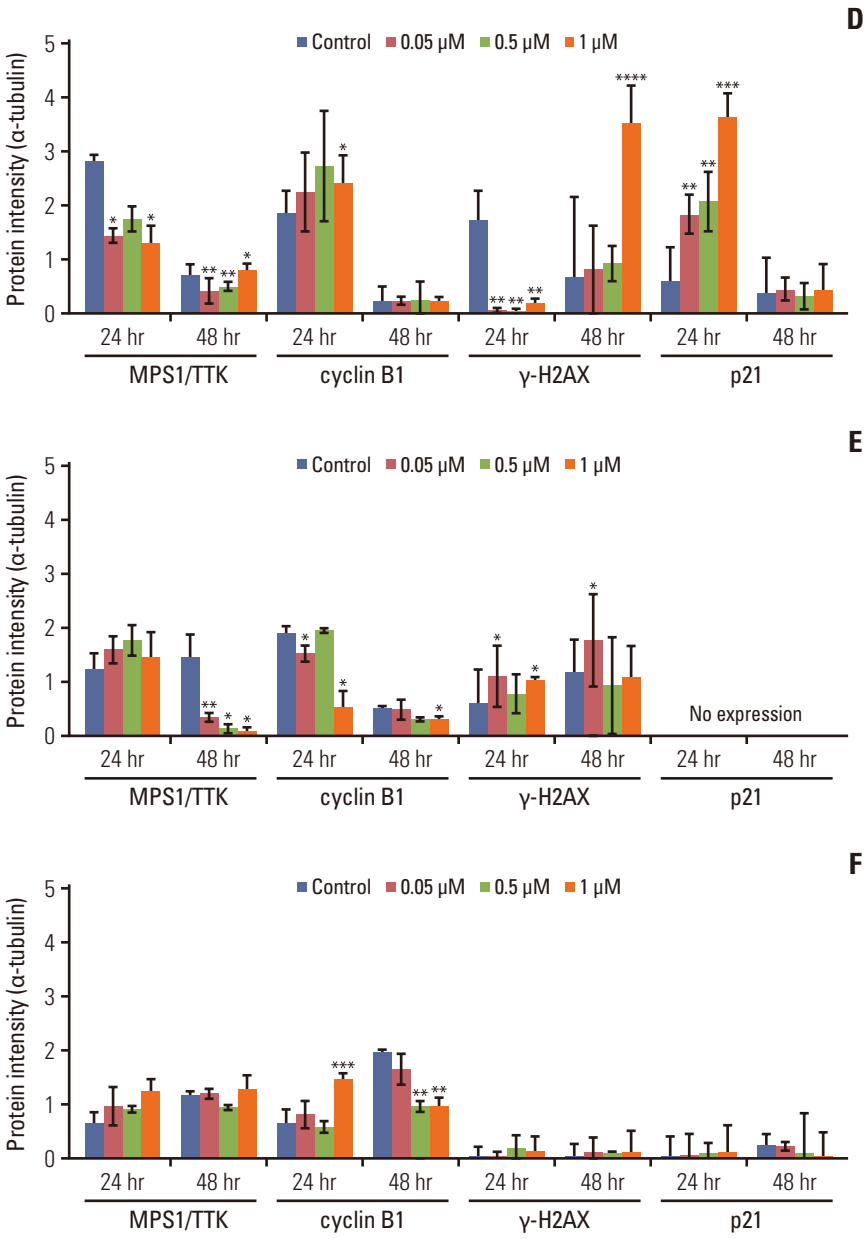

Fig. 4. *(Continued from the previous page)* Quantification of each western blot data is represented on YCC-47 cell line (D), YCC-30 cell line (E), and YCC-28 cell line (F). α-tubulin was used as a loading control for each experiment. All the statical test was compared to control group (blue) with the Wilcoxon matched-pairs signed rank test. Data are expressed as mean±standard error or mean; *$p < 0.05$, **$p < 0.01$, ***$p < 0.001$, ****$p < 0.0001$.

Following a 4-hour release from nocodazole, the G2/M arrest was reduced in YCC-47 cells, leading to increased aneuploidy and polyploidy, with some cells recovering to the G1 phase (Fig. 6A). In contrast, YCC-28 cells remained largely arrested in the G2/M phase, with limited polyploidy, and the recovery of these cells into the G1 phase was also observed (Fig. 6B). When treated with the MPS1/TTK inhibitor, YCC-47 cells failed to recover to the G1 phase, showing a significant increase in the sub-G1 population, indicating cell death (Fig. 6A). In contrast, YCC-28 cells did not exhibit an increase in the sub-G1 population and remained in the G2/M phase, suggesting resistance to the inhibitor's effects (Fig. 6B).

These results suggest that the MPS1/TTK inhibitor disrupted proper cell cycle recovery in YCC-47 cells following SAC activation, leading to cell death. In contrast, YCC-28 cells were able to proceed through the cell cycle and exhibit-

ed resistance to cell death induced by MPS1/TTK inhibition.

8. Changes in molecular factors after SAC activation in YCC-47 and YCC-28 cell lines following MPS1/TTK inhibition

In the previous paragraph, YCC-47 and YCC-28 cell lines were treated with nocodazole to induce SAC activation by arresting the cells in the G2/M phase. After release from nocodazole, we assessed molecular changes, including the expression levels of MPS1/TTK, cyclin B1, and phosphorylated or non-phosphorylated BUBR1, one of the downstream molecules of MPS1/TTK, in response to MPS1/TTK inhibitor (Fig. 7).

The expression levels of cyclin B1 and phosphorylated BUBR1 decreased with increasing concentration of the MPS1/TTK inhibitor in YCC-47 cell line (Fig. 7A and C). In contrast, cyclin B1 and phosphorylated BUBR1 expression levels increased in the YCC-28 (Fig. 7B and D) cell line, and then decreased after treatment with MPS1/TTK inhibitor concentrations up to 0.5 μM.

These results show that the MPS1/TTK inhibitor inhibited SAC activity in the YCC-47 cell line, resulting in mitotic catastrophe and cell death. However, SAC activity was maintained in the YCC-28 cell line.

Discussion

This study used compound-9, a highly selective MPS1/TTK inhibitor, to evaluate its anti-cancer effects on GC cell lines. Compound-9 demonstrated clear target specificity for MPS1/TTK, as evidenced by both kinase selectivity profiling and X-ray co-crystal structures [22]. In the kinase assay, Compound-9 exhibited an IC_{50} of 6.4 nM for MPS1/TTK and the thermal shift assay confirmed Compound-9's binding to MPS1/TTK, indicating a strong inhibitory effect and tight binding. These findings were supported by X-ray co-crystal analysis, which shows that Compound-9 directly binds to the ATP-binding pocket of MPS1/TTK, forming key interactions with residues such as K553 and D664. Additionally, Compound-9's efficacy has been shown to be comparable to that of CFI-402257, a well-known MPS1 inhibitor currently in Phase II clinical trials for advanced solid tumors and human epidermal growth factor receptor 2–negative breast cancer [22,28]. Compound-9 exhibited a similar level of pTTK (T33/S37) phosphorylation inhibition across multiple concentrations as CFI-402257. Compound-9 has demonstrated clear target specificity for MPS1/TTK, thereby supporting its role as a potent and selective inhibitor.

We further investigated the anti-cancer effects of MPS1/TTK inhibition, focusing on the suppression of MPS1/TTK

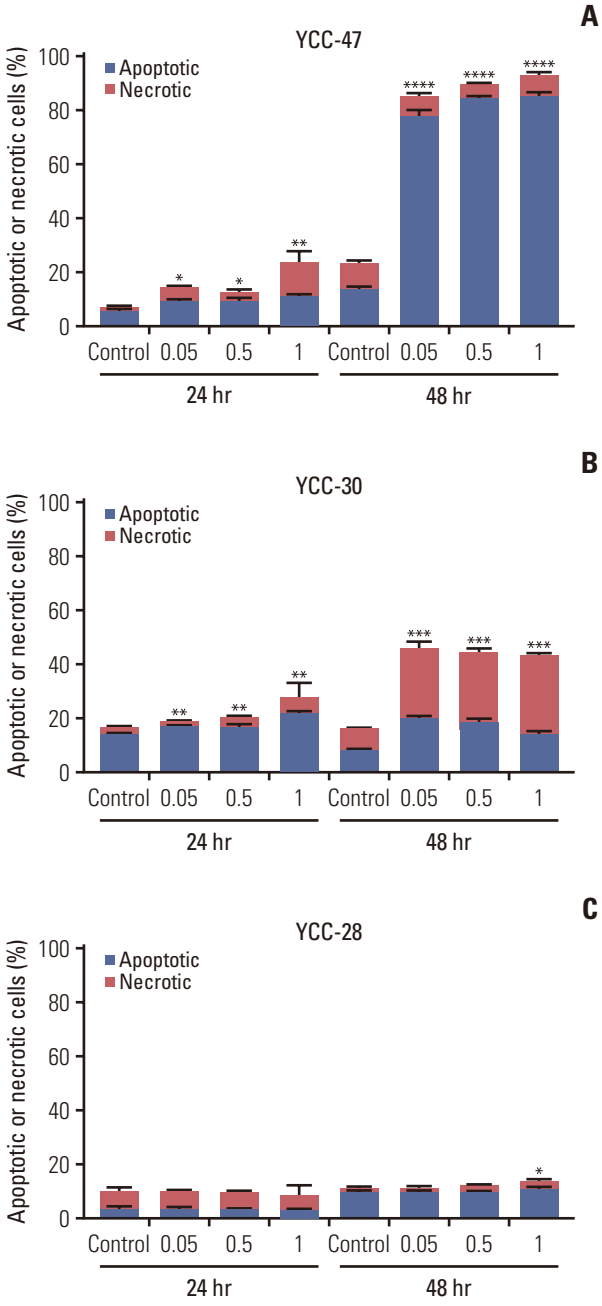

Fig. 5. Apoptosis induced by the monopolar spindle 1 (MPS1)/threonine tyrosine kinase (TTK) inhibitor. Representative flow cytometry plots obtained using annexin V–FITC/propidium iodide (PI) staining for apoptosis analysis in YCC-47 cell line (A), YCC-30 cell line (B), and YCC-28 cell line (C) (The y-axis represents % of apoptotic or necrotic cells, and the x-axis represents MPS1/TTK inhibitor concentrations). *(Continued to the next page)*

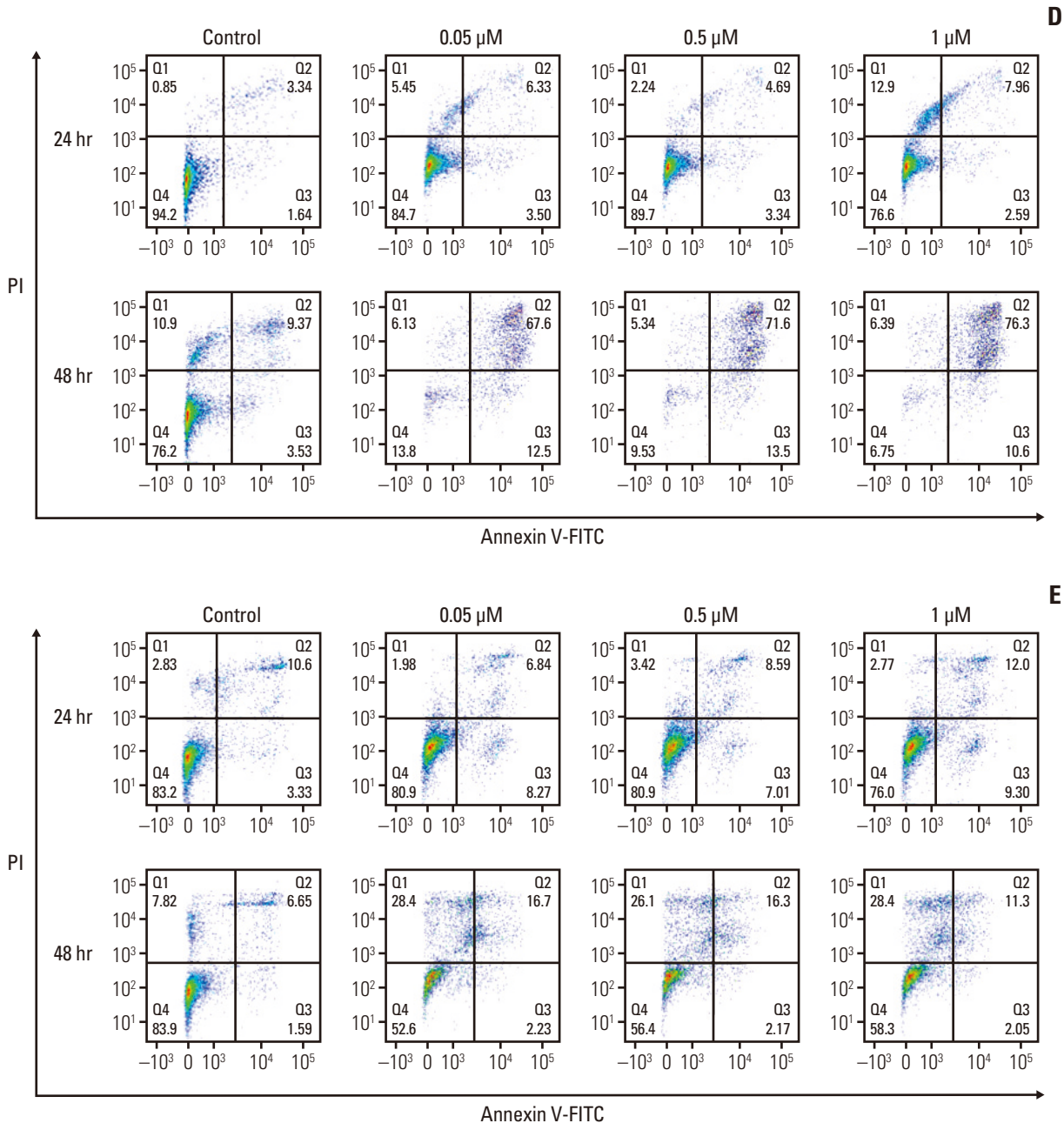

Fig. 5. *(Continued from the previous page)* Quantification of each apoptosis analysis data is represented on YCC-47 cell line (D), YCC-30 cell line (E), and YCC-28 cell line (F) (The y-axis represents PI, and the x-axis represents annexin V–FITC). All the statical test was compared to ctr group with the Wilcoxon matched-pairs signed rank test. Data are expressed as mean±standard error or mean; *$p < 0.05$, **$p < 0.01$, ***$p < 0.001$, ****$p < 0.0001$. *(Continued to the next page)*

autophosphorylation at the T33/S37 site in GC cell lines, and explored the underlying mechanisms. MPS1/TTK expression was analyzed in 408 GC tissues and 211 normal tissues in the TCGA data, and the results showed that MPS1/TTK was upregulated approximately 16-fold in GC [17]. According to the Human Protein Atlas database, the median TPM of MPS1/TTK mRNA is 28.4 in 42 GC cell lines, while the 61 GC panel used in this study have a median TPM of 39.1. We hypothesized that higher expression of the target molecule, MPS1/TTK, would make cells more sensitive to MPS1/TTK inhibitor; however, we found that at the cell line level, TPM values are low, and there is no correlation between MPS1/

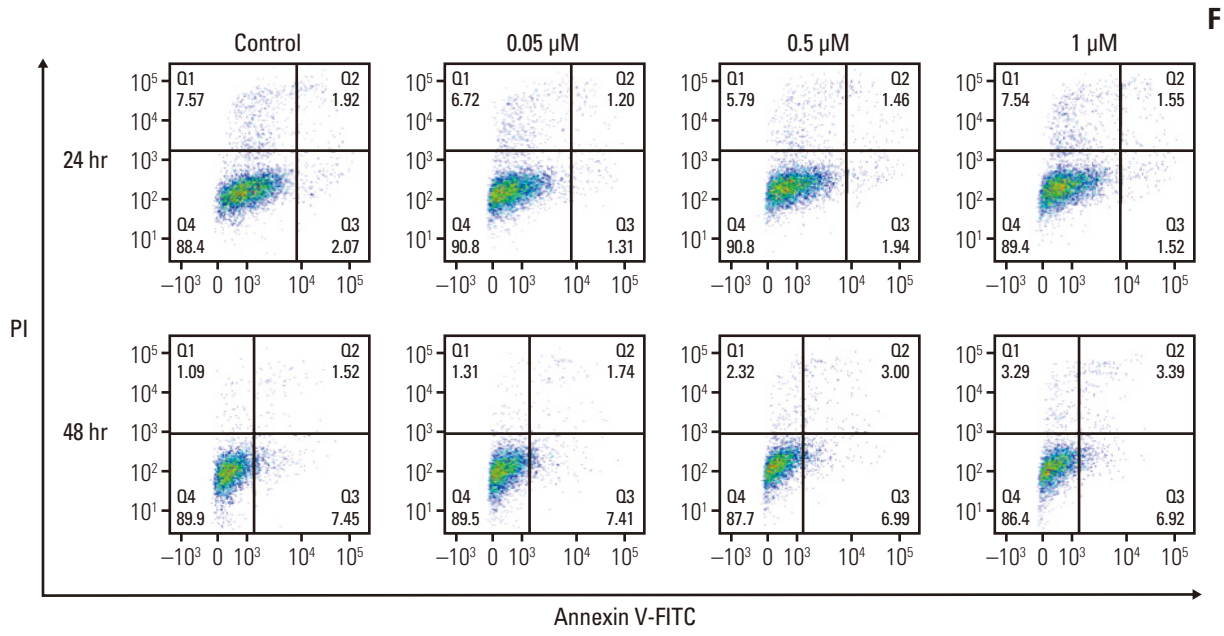

Fig. 5. *(Continued from the previous page)*

TTK expression levels and sensitivity to MPS1/TTK inhibitor (Fig. 2C and D).

Next, sensitivity to the MPS1/TTK inhibitor was analyzed based on TCGA subtypes. The CIN-likely group showed a tendency to be both sensitive and resistant to the MPS1/TTK inhibitor. Therefore, we concluded that a common feature of the sensitive cell lines in the CIN-likely group could serve as a biomarker for MPS1/TTK inhibition. The CIN-likely group was characterized by the amplification of genes encoding RTKs [25]. Interestingly, nine out of the 12 *MET*-amplified cell lines (9/12, 75%) were sensitive to the MPS1/TTK inhibitor. Previous studies reported that having an oncogenic MET receptor promoted centrosome amplification and increased CIN through the phosphoinositide 3-kinase–Akt pathway [29]. Therefore, further studies should establish the relationship between *MET* amplification and MPS1/TTK inhibitors, which may serve as biomarkers (Table 1).

Previous studies reported that an intact SAC is required for proper execution of the post-mitotic checkpoint, but the underlying mechanistic details remain unclear [30]. Therefore, we analyzed the TP53 status of 61 GC cell lines to assess the association between TP53 status and induction of apoptosis by MPS1/TTK inhibitor. The results suggest that when deleterious CIN is induced by MPS1/TTK inhibitor treatment, $TP53^{WT}$ group detects it and induces cell death, while $TP53^{MUT}$ group tolerates deleterious CIN and continues cell survival. However, these cell lines have high levels of chromosomal instability (CIN) and undergo several additional cell cycles compared to the $TP53^{WT}$ cell line, and they either undergo apoptosis or continue to survive.

Although the sample size was too small to analyze statistically significant conclusions, cell lines with mutations in DDR-related genes tended to exhibit more sensitive-to-moderate responses to MPS1/TTK inhibitor compared to those without such mutations (Table 1). This observation suggests a possible link between DDR gene mutations and sensitivity to MPS1/TTK inhibitors, indicating the presence of additional mechanisms driving this sensitivity. Further research is needed to clarify the interplay between SAC, the post-mitotic checkpoint, and DDR in managing genomic instability.

The findings of our study can be summarized in four points as follows. (1) We found that $TP53^{WT}$ cell lines in the CIN-likely group were sensitive to the inhibitor. (2) Among the 27 cell lines in the CIN-likely group, 12 had *MET* amplification, seven of which were sensitive to the MPS1/TTK inhibitor. (3) $TP53^{MUT}$ cell lines required more cell cycles than $TP53^{WT}$ and sensitive cell lines, suggesting that cell death occurs through TP53-independent mechanisms. (4) These cell lines likely possess a functioning DDR system, which requires further investigation.

In conclusion, this study explored the sensitivity of 61 GC cell lines to an MPS1/TTK inhibitor and identified the key factors associated with sensitivity to the inhibitor. Our results suggest that the CIN-likely subtype and TP53 wild-type status may serve as potential indicators of a sensitive response to the inhibitor.

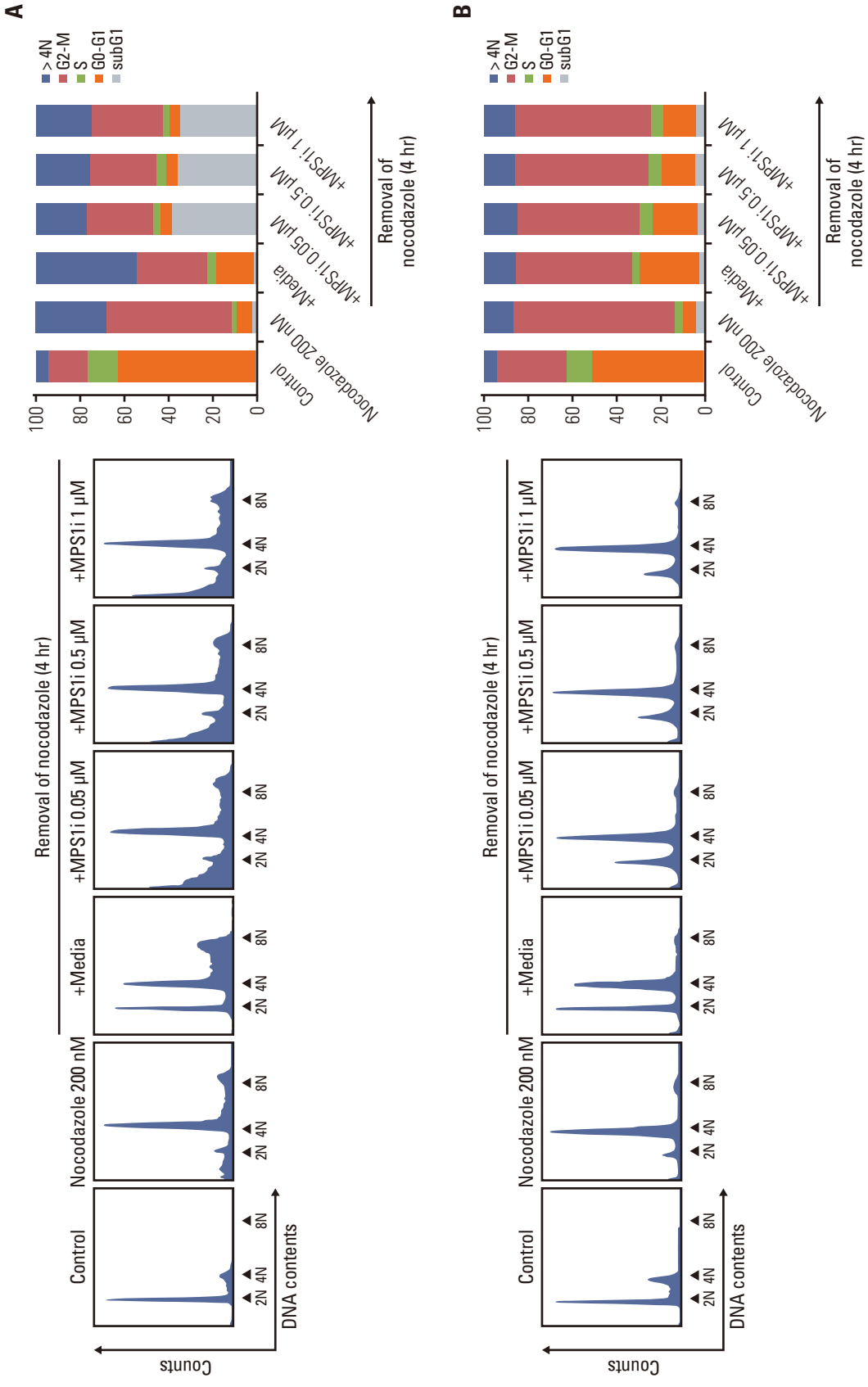

Fig. 6. Comparisons of inhibition of monopolar spindle 1 (MPS1)/threonine tyrosine kinase (TTK) function and spindle assembly checkpoint activity induced by the MPS1/TTK inhibitor. Effect of the MPS1/TTK inhibitor on cell-cycle progression in YCC-47 cell line (A) and YCC-28 cell line (B). At the left panel, histograms of cell cycle analysis were represented (The y-axis represents cell counts, and the x-axis represents DNA modal contents). At the right panel, cell cycle distribution bar graph were represented (The y-axis represents the percentage of cell population, and the x-axis represents the conditions). All the statical test was compared to media group with the Wilcoxon matched-pairs signed rank test.

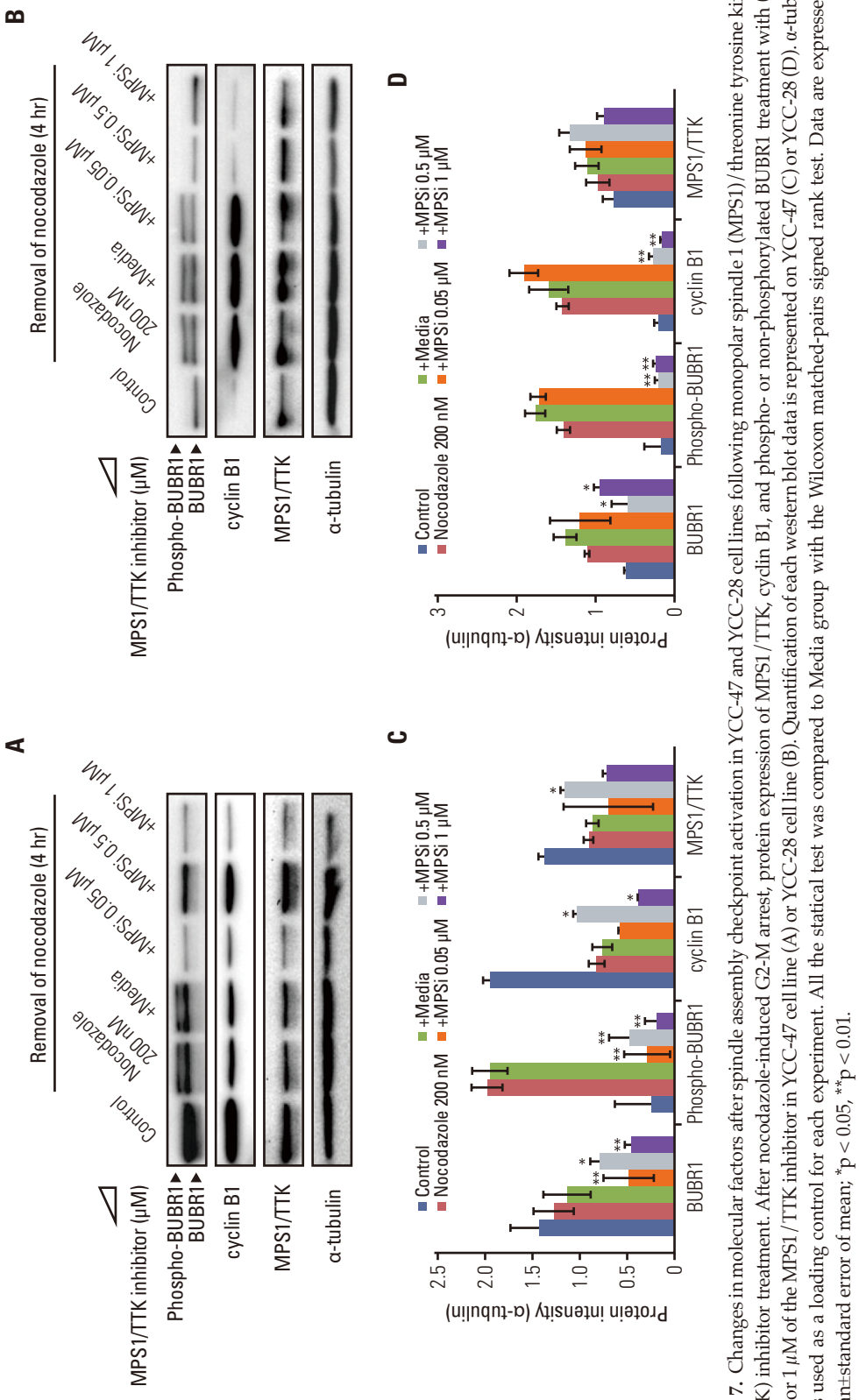

Fig. 7. Changes in molecular factors after spindle assembly checkpoint activation in YCC-47 and YCC-28 cell lines following monopolar spindle 1 (MPS1)/threonine tyrosine kinase (TTK) inhibitor treatment. After nocodazole-induced G2-M arrest, protein expression of MPS1/TTK, cyclin B1, and phospho- or non-phosphorylated BUBR1 treatment with 0.05, 0.5, or 1 μM of the MPS1/TTK inhibitor in YCC-47 cell line (A) or YCC-28 cell line (B). Quantification of each western blot data is represented on YCC-47 (C) or YCC-28 (D). α-tubulin was used as a loading control for each experiment. All the statical test was compared to Media group with the Wilcoxon matched-pairs signed rank test. Data are expressed as mean±standard error of mean; $^{*}p < 0.05$, $^{**}p < 0.01$.

Electronic Supplementary Material

Supplementary materials are available at Cancer Research and Treatment website (https://www.e-crt.org).

Author Contributions

Conceived and designed the analysis: Kim E, Kwon WS, Hwang J, Rha SY.

Collected the data: Kim E, Kwon WS, Hwang J.

Contributed data or analysis tools: Kim E, Kwon WS, Kim TS, Hwang J.

Performed the analysis: Kim E.

Wrote the paper: Kim E.

Conceptualization, resources, writing - review & editing, data curation, supervision, project administration, funding acquisition: Kim E, Kim TS, Kim S, Rha SY.

ORCID iDs

Eunseo Kim : https://orcid.org/0009-0004-7398-5928

Sun Young Rha : https://orcid.org/0000-0002-2512-4531

Conflicts of Interest

MPS1/TTK inhibitor was provided by Company (Voronoi Inc. Incheon, South Korea).

Funding

This study was supported by the National Research Foundation of Korea (NRF) grant funded by the Korea government (MSIT) (2020R1A2B5B02001452) and also supported by a grant from the National R&D Program for Cancer Control, Ministry of Health and Welfare, Republic of Korea (HA15C0005).

References

1. Thrift AP, Wenker TN, El-Serag HB. Global burden of gastric cancer: epidemiological trends, risk factors, screening and prevention. Nat Rev Clin Oncol. 2023;20:338-49.
2. Kang MJ, Jung KW, Bang SH, Choi SH, Park EH, Yun EH, et al. Cancer statistics in Korea: incidence, mortality, survival, and prevalence in 2020. Cancer Res Treat. 2023;55:385-99.
3. Wagner AD, Syn NL, Moehler M, Grothe W, Yong WP, Tai BC, et al. Chemotherapy for advanced gastric cancer. Cochrane Database Syst Rev. 2017;8:CD004064.
4. Maleki SS, Rocken C. Chromosomal instability in gastric cancer biology. Neoplasia. 2017;19:412-20.
5. Giam M, Rancati G. Aneuploidy and chromosomal instability in cancer: a jackpot to chaos. Cell Div. 2015;10:3.
6. Dhital B, Rodriguez-Bravo V. Mechanisms of chromosomal instability (CIN) tolerance in aggressive tumors: surviving the genomic chaos. Chromosome Res. 2023;31:15.
7. Musacchio A, Salmon ED. The spindle-assembly checkpoint in space and time. Nat Rev Mol Cell Biol. 2007;8:379-93.
8. Lara-Gonzalez P, Westhorpe FG, Taylor SS. The spindle assembly checkpoint. Curr Biol. 2012;22:R966-80.
9. Yuan B, Xu Y, Woo JH, Wang Y, Bae YK, Yoon DS, et al. Increased expression of mitotic checkpoint genes in breast cancer cells with chromosomal instability. Clin Cancer Res. 2006;12:405-10.
10. Maire V, Baldeyron C, Richardson M, Tesson B, Vincent-Salomon A, Gravier E, et al. TTK/hMPS1 is an attractive therapeutic target for triple-negative breast cancer. PLoS One. 2013;8:e63712.
11. Maachani UB, Kramp T, Hanson R, Zhao S, Celiku O, Shankavaram U, et al. Targeting MPS1 enhances radiosensitization of human glioblastoma by modulating DNA repair proteins. Mol Cancer Res. 2015;13:852-62.
12. Tannous BA, Kerami M, Van der Stoop PM, Kwiatkowski N, Wang J, Zhou W, et al. Effects of the selective MPS1 inhibitor MPS1-IN-3 on glioblastoma sensitivity to antimitotic drugs. J Natl Cancer Inst. 2013;105:1322-31.
13. Lin J, Shi J, Guo H, Yang X, Jiang Y, Long J, et al. Alterations in DNA damage repair genes in primary liver cancer. Clin Cancer Res. 2019;25:4701-11.
14. Landi MT, Dracheva T, Rotunno M, Figueroa JD, Liu H, Dasgupta A, et al. Gene expression signature of cigarette smoking and its role in lung adenocarcinoma development and survival. PLoS One. 2008;3:e1651.
15. Slee RB, Grimes BR, Bansal R, Gore J, Blackburn C, Brown L, et al. Selective inhibition of pancreatic ductal adenocarcinoma cell growth by the mitotic MPS1 kinase inhibitor NMS-P715. Mol Cancer Ther. 2014;13:307-15.
16. Salvatore G, Nappi TC, Salerno P, Jiang Y, Garbi C, Ugolini C, et al. A cell proliferation and chromosomal instability signature in anaplastic thyroid carcinoma. Cancer Res. 2007;67:10148-58.
17. Huang H, Yang Y, Zhang W, Liu X, Yang G. TTK regulates proliferation and apoptosis of gastric cancer cells through the Akt-mTOR pathway. FEBS Open Bio. 2020;10:1542-9.
18. Margolis RL, Lohez OD, Andreassen PR. G1 tetraploidy checkpoint and the suppression of tumorigenesis. J Cell Biochem. 2003;88:673-83.
19. Rieder CL, Maiato H. Stuck in division or passing through: what happens when cells cannot satisfy the spindle assembly checkpoint. Dev Cell. 2004;7:637-51.
20. Lanni JS, Jacks T. Characterization of the p53-dependent postmitotic checkpoint following spindle disruption. Mol Cell Biol. 1998;18:1055-64.
21. Meek DW. The role of p53 in the response to mitotic spindle damage. Pathol Biol (Paris). 2000;48:246-54.
22. Lee Y, Kim H, Kim H, Cho HY, Jee JG, Seo KA, et al. X-ray crystal structure-guided design and optimization of 7H-pyrrolo[2,3-d]pyrimidine-5-carbonitrile scaffold as a potent and orally active monopolar spindle 1 inhibitor. J Med Chem.

2021;64:6985-95.
23. Kwon WS, Che J, Rha SY, Chung HC, Han HJ, Kim J, et al. Development and validation of a targeted sequencing panel for application to treatment-refractory solid tumor. J Clin Oncol. 2021;39(3 Suppl):245.
24. Kim HJ, Kang SK, Kwon WS, Kim TS, Jeong I, Jeung HC, et al. Forty-nine gastric cancer cell lines with integrative genomic profiling for development of c-MET inhibitor. Int J Cancer. 2018;143:151-9.
25. Cancer Genome Atlas Research Network. Comprehensive molecular characterization of gastric adenocarcinoma. Nature. 2014;513:202-9.
26. Niittymaki I, Gylfe A, Laine L, Laakso M, Lehtonen HJ, Kondelin J, et al. High frequency of TTK mutations in microsatellite-unstable colorectal cancer and evaluation of their effect on spindle assembly checkpoint. Carcinogenesis. 2011;32:305-11.
27. Hwang J, Kwon WS, Park J, Bae HJ, Jeong I, Kang SK, et al. Evaluation of DNA damage repair gene alterations, microsatellite instability status, and tumor mutational burden as predictive biomarkers of olaparib sensitivity in gastric cancer. Cancer Res. 2021;81(13_Suppl):2055.
28. Mason JM, Wei X, Fletcher GC, Kiarash R, Brokx R, Hodgson R, et al. Functional characterization of CFI-402257, a potent and selective Mps1/TTK kinase inhibitor, for the treatment of cancer. Proc Natl Acad Sci U S A. 2017;114:3127-32.
29. Nam HJ, Chae S, Jang SH, Cho H, Lee JH. The PI3K-Akt mediates oncogenic Met-induced centrosome amplification and chromosome instability. Carcinogenesis. 2010;31:1531-40.
30. Vogel C, Kienitz A, Hofmann I, Muller R, Bastians H. Crosstalk of the mitotic spindle assembly checkpoint with p53 to prevent polyploidy. Oncogene. 2004;23:6845-53.